

# Deakin Research Online

**This is the published version:**

Sugumar, D., Ismail, Asma, Ravichandran, Manickam, Aziah, Ismail and Kong, L. X. 2010, Amplification of SPPS150 and salmonella typhi DNA with a high throughput oscillating flow polymerase chain reaction device, *Biomicrofluidics*, vol. 4, no. 2, pp. 1-12.

**Available from Deakin Research Online:**

<http://hdl.handle.net/10536/DRO/DU:30028499>

Reproduced with the kind permission of the copyright owner.

**Copyright** : 2010, American Institute of Physics

## Amplification of SPPS150 and *Salmonella typhi* DNA with a high throughput oscillating flow polymerase chain reaction device

D. Sugumar,<sup>1,2,a)</sup> Asma Ismail,<sup>3</sup> Manickam Ravichandran,<sup>4</sup> Ismail Aziah,<sup>3</sup> and L. X. Kong<sup>1,a)</sup>

<sup>1</sup>Centre for Material and Fibre Innovation, Deakin University, Waurn Ponds Campus, Geelong, 3217 Victoria, Australia

<sup>2</sup>Faculty of Manufacturing Engineering, Technical University Malaysia Melaka, 76109 Durian Tunggal, Melaka, Malaysia

<sup>3</sup>Institute for Research in Molecular Medicine (INFORMM), University Sains Malaysia, Health Campus, Kubang Kerian, 16150 Kelantan, Malaysia

<sup>4</sup>Asian Institute of Medicine, Science and Technology (AIMST), Semeling, 08100 Kedah, Malaysia

(Received 3 February 2010; accepted 9 April 2010; published online 3 May 2010)

In this paper, a novel oscillating flow polymerase chain reaction (PCR) device was designed and fabricated to amplify *SPPS150* and *salmonella typhi*. In this new design, the samples are shuttled (oscillating flow) inside a microfluidic chip to three different temperature zones required for DNA amplification. The amplification cycle time has markedly been reduced as the reagent volume used was only about 25% of that used in conventional PCRs. Bubble formation and adsorption issues commonly associated to chip based PCR were also eliminated. Based on the performance evaluated, it is demonstrated that this oscillating flow PCR has the advantages of both the stationary chamber and continuous flow PCR devices. © 2010 American Institute of Physics. [doi:10.1063/1.3422524]

### I. INTRODUCTION

In the past decade there has been an increased demand for rapid and accurate detection of pathogenic bacteria, viruses, and other disease causing agents. The improvement in molecular diagnostics and the better understanding of the human genome have led to a new concept of medicine, in which molecular diagnosis plays a central role. Early detection with molecular biology can also predict how patients will respond to particular forms of treatment.<sup>1</sup> Molecular diagnostics such as polymerase chain reaction (PCR) technologies have played an increasingly important role in healthcare. They are able to detect diseases early, stratify patients for treatment, and render high treatment success rate. However, they have a slow response to results, cannot perform amplifications of multidiseases or samples, and are bulky and not portable, even with the relatively advanced PCR technologies.

PCR was first performed in multiple water baths<sup>2</sup> and then in programmable heat blocks or thermal cyclers.<sup>3-5</sup> It offered an increased performance for clinical laboratories. With the advancement in the microelectromechanical system technology, miniaturized PCR devices superior to the conventional PCR devices have been developed since the early 1990s.<sup>6-10</sup> The advantages of miniaturized PCR were first mooted by the pioneering work of Wittwer *et al.*<sup>11</sup> Although the original work of Wittwer did not mention anything about PCR chips, the underlying idea presented inspired Northrup *et al.*<sup>12</sup> to develop a silicon based PCR chip that became a major milestone in

<sup>a)</sup>Authors to whom correspondence should be addressed. Electronic addresses: sugumar@utem.edu.my and lingxue.kong@deakin.edu.au.

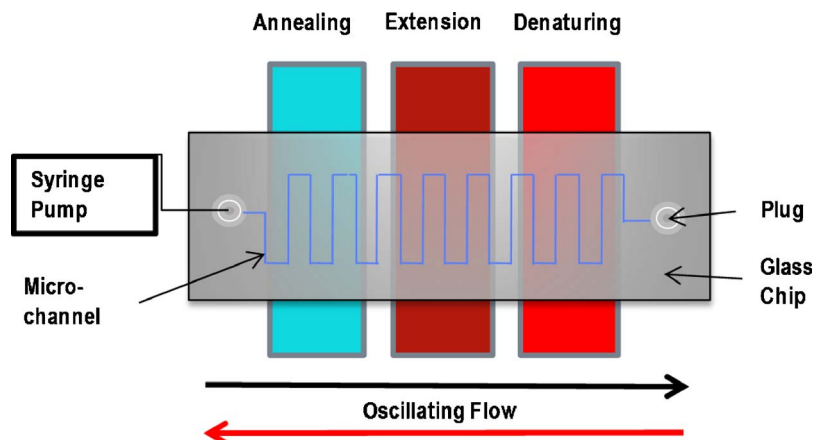


FIG. 1. Schematic of oscillating flow PCR (not to scale).

molecular diagnostics. Since then, many types of PCR chips have been introduced; the two most researched formats are the stationary chamber and continuous flow PCR devices.

The major advantages demonstrated by these two formats are reduced cycle time and reduced sample usage compared to a conventional device. However, these PCR chips use substrate materials, such as silicon that require the employment of expensive and sophisticated fabrication processes, leading to a very high unit price. Furthermore, as a result of increased surface to volume ratio (SVR) and the type of materials used,<sup>6,13</sup> some effects not very common with the conventional PCRs become significant, including nonspecific adsorption of biological samples, inhibition, sample evaporation, and formation of bubbles.

It is important to develop a temperature cycling reaction microchip that integrates stationary chamber and continuous flow PCRs. In an integrated system introduced in the current work, efficient temperature cycling of the flow-through microchannel PCR chip can be performed, while the flexibility of varying the cycle number and the number of temperature zones in the stationary chamber PCR chip is maintained. The efficiency of the hybrid PCR device is validated by successfully detecting SPPS150 and *Salmonella typhi*. Issues related to sample inhibition, adsorption, and bubble formation are also comprehensively evaluated.

## II. OSCILLATING FLOW CONCEPT

Temperature cycling using a fixed temperature gradient involves pumping the PCR sample plug along the microchannel and shuttling it back and forth between microchannel zones of designated temperatures (Fig. 1). The precise control of sample movement in three different temperature zones is vital to improve efficiency. The sample movement was regulated with a syringe pump by applying required hydrostatic pressure. A positive pressure was first applied in the channel, driving the PCR sample plug within the microchannel. In order to pull back the sample plug to its original position in the chip, a negative pressure is then applied. The advantage of this amplification system is that the number of cycles can be actively manipulated compared to continuous flow PCR chips. Furthermore, the chip can be modified to create multiple channels and run several tests concurrently.

Since the PCR chips and the heating elements are fabricated separately, various channel designs can be fitted to the same heating elements to obtain different temperature cycling parameters. Alternatively, different temperature cycling schemes can be obtained without modifying the chip by means of an appropriate sample pumping scheme. Under the latter approach, when performing the temperature cycling reaction process, the sample can be shuttled at different pumping speeds to change the temperature ramping rate. The sample plug can also be maintained in a stationary position so that it is incubated at a constant temperature associated with that particular location.

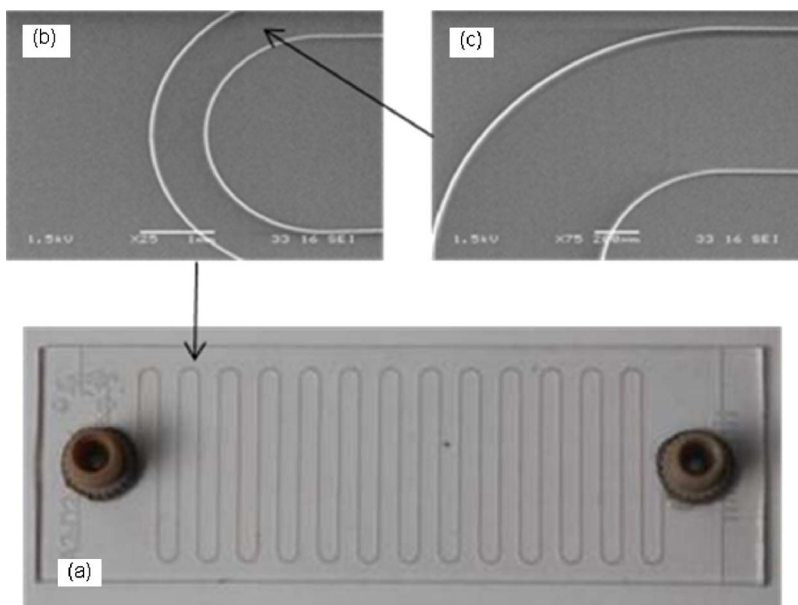


FIG. 2. (a) Fabricated glass chip with nanoports attached to the access holes. (b) and (c) SEM of the microchannel bends.

### A. Chip design and fabrication

The glass chip was designed based on the more established continuous flow PCR chip.<sup>10,14–16</sup> In the oscillating flow PCR system the temperatures in the denaturing, annealing, and extension zones were kept constant over time while the sample was moving through these individual zones (Fig. 1). According to Fick's law,<sup>10</sup> the time needed for heat dissipation is directly proportional to the second power of the channel depth for a flat rectangular channel, assuming that the thermostated copper blocks and chip represent an infinite heat capacity relative to the heated fluid element. Hence, the time delay for the sample to reach a new temperature depends only on the time needed to transport the sample into the appropriate temperature zone as heating a fluid element in the capillary is very quick.<sup>10</sup>

The PCR efficiency is directly associated with the heat transfer rate during the heating and cooling processes. As there is an average of 30 cycles in each test, a reduction in the time consumed in each cycle will lead to a significant improvement in overall efficiency accumulated from optimized heating. The length of the chip was also optimally designed to allow for only one complete amplification cycle and to reduce the volume of sample being used. The extension zone was arranged in the chip center between the denaturing and the annealing zones (Fig. 1). The dimension of the glass chip is  $30 \times 90$  mm<sup>2</sup> that is the standard size of a borofloat glass. The fluid channel comprises a serpentine channel with a width of 500  $\mu\text{m}$ , depth of 100  $\mu\text{m}$ , and a total length of 696 mm. The total volume of the channel is about 35  $\mu\text{l}$ . This effectively provides a SVR of about 24.

The PCR chip was fabricated from borofloat glass sheets by Micronit Microfluidics BV, Netherlands. The channels were etched on a glass chip with a thickness of 0.7 mm and the access holes were fabricated on a 1.1 mm thickness glass chip. The microchannels inside the glass were created by using the deep reactive ion etching technique. The access holes were fabricated using the powder blasting technique. Finally the chip cover was bonded to the chip at a high temperature. The bond was strong enough to sustain a pressure up to 150 bars [Fig. 2(a)]. A magnified top view of the channel radius and curvature is shown in the scanning electron micrograph (SEM) photographs [Figs. 2(b) and 2(c)].

It is desirable that the surface of the microchannels in the PCR chip is hydrophobic or modified with a coating that prevents adsorption of small molecules during PCR

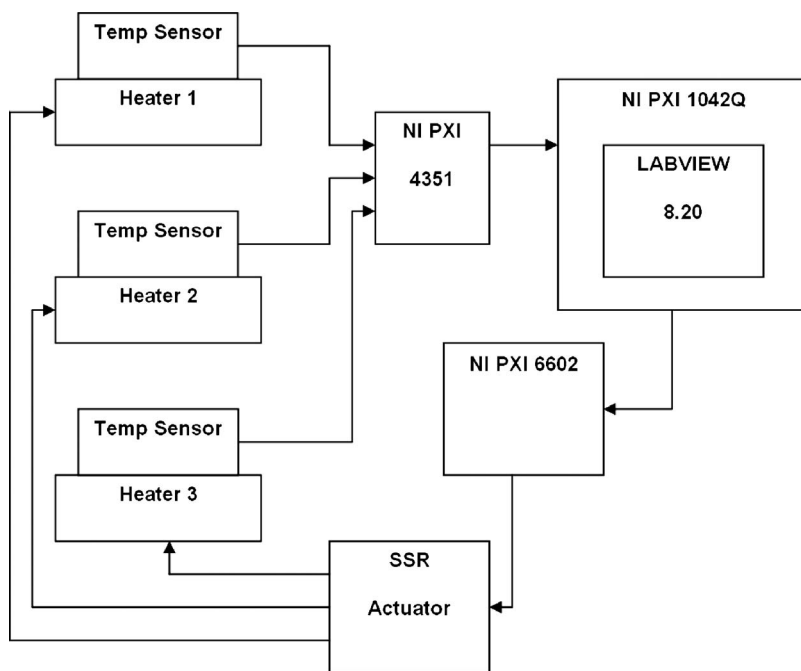


FIG. 3. Schematic of the temperature control system.

applications.<sup>8,13,17,18</sup> By using a proprietary ultrathin surface treatment method, the glass surface in the channels was modified (Micronit BV), creating hydrophobic surfaces on channel walls. The coating on the microchannel walls also reduces the surface energy in order to ensure that the liquid sample forms a unified plug when pumped through the channel. To provide access to the channel, two 10-32 Coned Nanoport Assemblies (UpChurch Scientific, F-333N, WA, USA) able to accommodate 1.60 mm tubing (outside diameter) were bonded to the powder blasted holes on the upper glass chip layer. Figure 2(a) shows the assembled glass chip with the two nanoports attached.

## B. Heating system

In addition to the PCR chip, heating system is the other main component of this oscillating flow PCR device. The heating system has cartridge heaters, aluminum blocks, thermistors for heat sensing, a power supply unit with solid state relays (SSRs), and a National Instruments (NI) control system to control the temperatures. Figure 3 shows the schematic of the heating system for this setup. The temperature measurement and control system comprises thermistors, NI PXI 4351 data acquisition card, and LABVIEW for closed-loop temperature control. The thermistors were attached to the heater blocks with heat conducting epoxy glue. NI PXI-6602 counter/timer data acquisition card was used that controls the SSR actuator directly connected to the heaters. To ensure good thermal contact of the PCR chip with the aluminum heater blocks, the chip was pressed against the flat surface of the heater blocks by using nylon bolts fastened through the acrylic support plate. The support plate was also used as a guide to position a probe temperature sensor to acquire localized temperature on the surface of the glass chip. An additional thin layer of silicone heat transfer compound (Unick Chemical Corp., USA) was applied between the heater blocks and the glass chip to further enhance the thermal contact. Figure 4 shows the full experimental setup of the oscillating flow PCR device.



FIG. 4. PCR chip system setup. (1) PCR glass chip, (2) syringe pump, (3) glass syringe, (4) fluidic connections, (5) temperature control system, and (6) heater housing with temperature sensors.

### III. MATERIALS AND EXPERIMENTAL

#### A. Sample preparation

To validate the design, two types of DNA samples were utilized. The amplification of SPPS150 and *Salmonella typhi* produces 150 and 1238 bp amplicons as a final product, respectively. Table I lists the composition of the PCR samples. To compare DNA amplification using the chip based device, a standard protocol PCR product was prepared using MJ Research PTC-200. Table II provides the standard PCR temperature protocol and cycle setup using the conventional thermal cycler. The cycle time for the amplification of both SPPS150 and *Salmonella typhi* with MJ Research PTC-200 is 90 and 105 min, respectively.

#### B. Experimental setup

5  $\mu$ l PCR mix was introduced inside the oscillating PCR chip with standard *Eppendorf* micropipettes. The sample flowed inside the microchannel due to strong capillary effect that can fill up less than 1/3 of the total channel length, while the other 2/3 of the channel length is used as a buffer zone to enable the sample to be oscillated within the channel. In order to avoid sample evaporation upon loading, the samples were loaded at the annealing zone with a temperature lower

TABLE I. Composition of different PCR mixtures.

Components	Concentration		Volume ( $\mu$ l)
	SPPS150	<i>S. typhi</i>	
PCR buffer with (NH <sub>4</sub> ) <sub>2</sub> SO <sub>4</sub>		1 $\times$	2.0
MgCl <sub>2</sub> (mM)		2.5	2.0
dNTPs (mM)		0.16	0.32
Forward primer (pmole/ $\mu$ l)	1	10	1.0
Reverse primer (pmole/ $\mu$ l)	1	10	1.0
<i>Taq</i> DNA polymerase (U/ $\mu$ l)		0.75	0.15
Enzyme stabilizer		6%	2.4
dH <sub>2</sub> O			9.13
DNA template			2.0
Total			20.0

TABLE II. Standard PCR temperature and cycle setup using conventional thermal cycler.

Step	Temperature (°C)	Time		Cycles
		SPPS150	<i>S. typhi</i>	
Initial denaturation	95	3 min	3 min	1
Denaturation	95	30 s	30 s	30
Annealing	<i>T<sub>a</sub></i>	30 s	30 s	30
Elongation	72	30 s	1 min	30
Average cycle time		90s	120 s	30
Final annealing	<i>T<sub>a</sub></i>	30 s	30 s	1
Final extension	72	5 min	10 min	1
Total cycle time		90 min	105 min	30

than 65 °C. Following sample loading, an NE-1000 programmable syringe pump that controls the sample oscillation was connected to the port near the annealing temperature zone using *Upchurch Scientific* fluidic connectors and tubing. The air pressure was supplied by using a *SGE* glass syringe with a volume of 5 ml attached to the NE-1000 syringe pump. The other port was closed using a plug.

To control the sample plug movement inside the glass chip, pressurized air was pumped into the channel through a glass syringe (*SGE*, Australia) attached to the syringe pump to move the liquid forward into the microchannel. When the pressure inside the syringe is reduced (by reversing the action of the pumping direction), the liquid plug is pulled back toward the initial position inside the chip.

PCR samples were prepared in a 20  $\mu$ l reaction mixture volume. The anticipated product lengths are 150 and 1238 bp, calculated from the primer alignment to the template sequence. The initial pumping rate was set to 30  $\mu$ l/s to oscillate the sample plug inside the glass chip. The pumping rate and the number of temperature cycles were controlled by the programmable syringe pump. After the temperature cycling, 4–4.5  $\mu$ l of the amplified product was retrieved from the loading port of the glass chip with a micropipette. The amplified PCR samples were then electrophoresed through a 1.5% agarose gel (*Promega*, USA) stained with ethidium bromide (final concentration of 0.5  $\mu$ g/ml) in tris-acetate 1X buffer and then visualized under UV light.

### C. Inhibition and adsorption experiments

When glass chips are used, sample inhibition and adsorption can be a major issue if the surfaces of the microchannels are not well prepared.<sup>13,17,19,20</sup> The surface adsorption of PCR components toward the chip wall is due to the huge increase in the SVR in PCR chips. Also DNA and *Taq* polymerase both as polar molecules could be theoretically adsorbed to bare glass chips, posing a problem in PCR inefficiency. Hence in the light of previously observed adsorption problem, it was decided to first carry out a series of off-chip experiments to separately assess the adsorption problems and then proceed to gauge the adsorption issues on the PCR chip used, if indeed exist. The channels in the glass PCR chip were coated with a thin layer of fluorinated carbon (proprietary polymer coating of *Micronit BV*) to reduce or eliminate adsorption of molecules to the channel wall.

Since either DNA or polymerase molecules could be actively adsorbed to the wall of the PCR chips, initial batches of experiments were carried out to determine whether DNA was being actively adsorbed. In a standard PCR mix, there are three types of DNA molecules present: template DNA, primers, and free oligonucleotides (*dNTPs*). An excessively low concentration of any of these three components can result in poor PCR amplification. However, template DNA was the most critical DNA in terms of adsorption since a lowered concentration of template at the initial stage of PCR would yield a poor efficiency, while primers and *dNTPs* should act more indirectly via a net effect on specificity.

TABLE III. Experimental schemes for process optimization.

	Scheme 1	Scheme 2	Scheme 3	Scheme 4
Initial stage (s)	120	120	120	120
Annealing (s)	30	20	10	10
Extension (s)	30	20	10	20
Denaturing (s)	30	20	10	10
Average cycle time (s)	105	75	45	55
Total time (min, 30 cycles)	54.5	39.5	24.5	29.5

A standard PCR mix without *Taq* polymerase was prepared and inserted into the PCR chip for 5–20 min at 4 °C. A total volume of 20  $\mu$ l was inserted into the glass chip using Eppendorf micropipettes. Afterward, the PCR mix was extracted and deposited into a standard PCR tube into which *Taq* polymerase was added and PCR was carried out using the conventional thermocycler and protocol. In order to reuse the chip, it was washed by flushing the chip with 50 ml of pressure driven distilled water and dried with N<sub>2</sub> flow between mix insertions.

Similar procedures developed for DNA template adsorption experiments were also used for *Taq* polymerase adsorption experiment. The same glass chip was used and flushed thoroughly with distilled water before being used. The PCR mix with *Taq* polymerase was inserted into the PCR chip using the standard Eppendorf micropipettes (20  $\mu$ l volume). The samples were incubated inside the chip for 5–25 min in total at 4 °C. Then the samples were extracted from the chip and again amplified using the standard thermocycler and protocols as per the DNA template experiments.

#### D. Bubble formation and adsorption experiments

Sample evaporation is often a major problem in microfluidic PCR devices because of low volume samples being used. A sample pumping scheme is devised in this study to reduce sample loss during the temperature cycling process. Another common problem related to PCR microfluidic is the formation of bubbles at elevated temperatures particularly during the denaturing cycle.<sup>21</sup> Oil plugs were introduced to reduce the bubble formation.

### IV. RESULTS AND DISCUSSION

#### A. PCR results

To determine optimal time required for the microfluidic PCR system to successfully amplify a DNA sample with a low product length (150 bp product), three schemes were initially employed (Table III). The procedures used were the same.

- (1) The sample plug was first positioned at the denaturing zone (95 °C) for 120 s.
- (2) Then the PCR sample was oscillated between different temperature zones by keeping the sample stationary at each temperature zone of denaturing, annealing, and extension zones for 30 s (scheme 1), 20 s (scheme 2), or 10 s (scheme 3).
- (3) The sample plug then pumped toward the denaturing zone again and a new cycle commenced with a cycle time of 105, 75, and 45s for schemes 1–3, respectively, including the time required to shuttle the sample to three different temperature zones.

Therefore, it takes about 54.5 min for scheme 1, 39.5 min for scheme 2, and 24.5 min for scheme 3 to complete 30 cycles of amplification (Table III).

Figure 5(a) presents the agarose gel electrophorogram of the amplified PCR product for scheme 1. The first lane indicates the 100 bp DNA ladder, the second lane shows the PCR product from conventional PCR machine, and the third lane is the PCR product from the chip. It can be seen that the chip successfully amplified the target 150 bp *SPSS150* DNA. The reaction time is approximately 54.5 min for the oscillating flow PCR device compared to 90 min using the con-

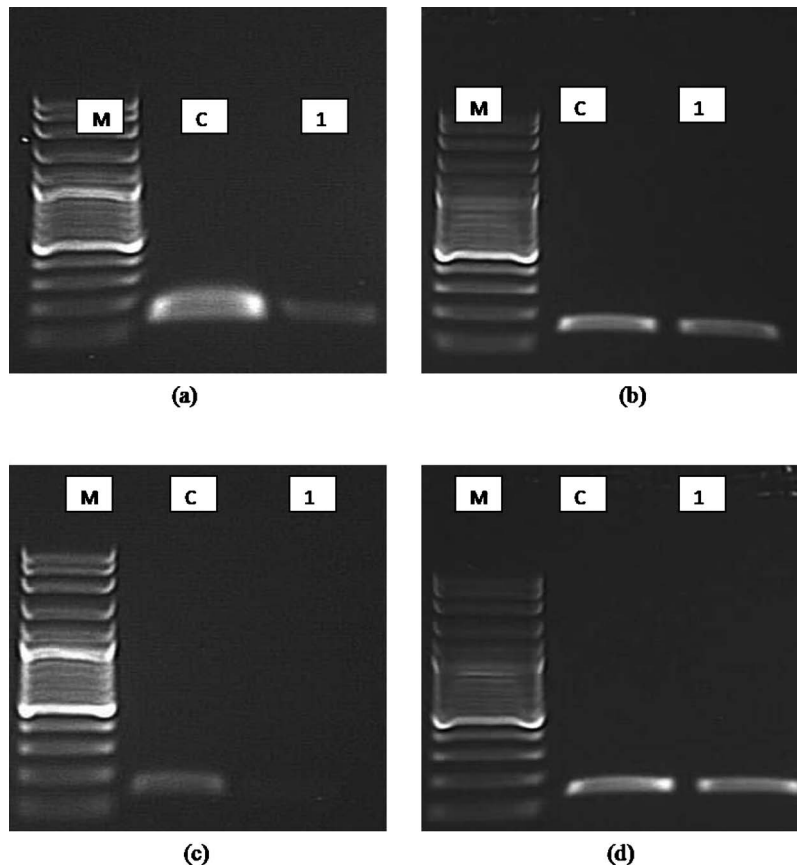


FIG. 5. Agarose gel electrophoresis of amplified 150 bp PCR product for cycle times of (a) 52.5, (b) 37.5, (c) 22.5, and (d) 29.5 min for 30 cycles (lane M: 100 bp ladder; lane C: control; lane 1: chip).

ventional PCR device, indicating that significant reduction in reaction time has been achieved.

When the reaction time reduced from 54.5 min (scheme 1) to 39.5 min (scheme 2), the efficiency of the 150 bp amplification [Fig. 5(b)] is slightly better when compared to Fig. 5(a). This demonstrates that a shorter dwelling time in each zone actually improves the amplification efficiency. The lower amplification efficiency with a much longer dwelling time can be attributed to the rapid deterioration of *Taq* polymerase at the denaturing temperature zone.

However, further reduction in the dwelling time in each zone (scheme 3) could lead to a deterioration of the DNA amplification efficiency. When the dwelling time was only 10 s each for denaturing, extension, and annealing zones, the amplification rate was very poor compared to those of schemes 1 and 2 [Fig. 5(c)].

Therefore, an optimal period of time is required for each temperature zone by considering the functions of these zones in order for the PCR sample to be successfully amplified. If denaturation time is too long, the *Taq* polymerase will be degraded while a short extension time decreases the ability for the extension process to complete its cycle efficiently. It is therefore inadequate to have an even timing as this may degrade the *Taq* polymerase and/or not complete the extension process.

Based on the experimental results observed from schemes 1–3, a new scheme (scheme 4, Table III) was introduced where a short time of 10 s for both the denaturing and annealing zones was adopted and a longer extension time of 20 s was employed. For this configuration, it takes about 55 s to complete each cycle and a total of 29.5 min to complete 30 cycles. The DNA was successfully amplified as demonstrated from the agarose gel electrophoresis of the amplified PCR product [Fig. 5(d)]. Therefore, the optimal reaction time for the 150 bp DNA templates is

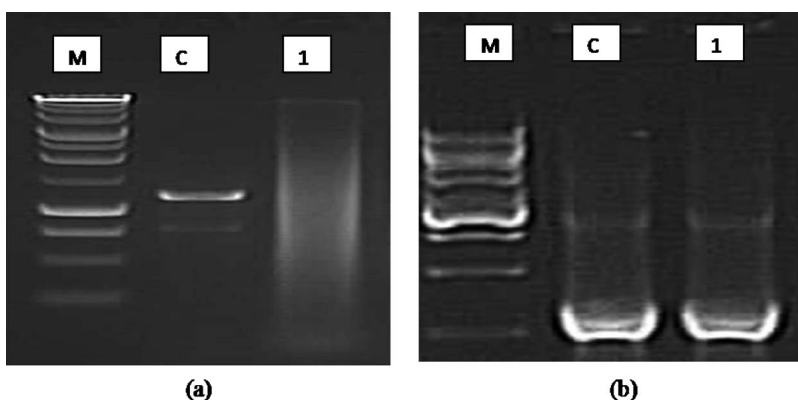


FIG. 6. Agarose gel electrophoresis of the amplified 1238 bp PCR product for cycle times of (a) 39.5 and (b) 55 min for 30 cycles (lane M: 1 kbp ladder; C: control; 1: chip).

29.5 min with short denaturing and annealing durations but with a much longer extension time. This is about one-third of the time required for amplifying 150 bp DNA templates using the conventional PCR devices (90 min).

To examine the robustness of the oscillating microfluidic PCR device, the much longer DNA template of *Salmonella typhi* with 1238 bp product was also tested. In conventional PCR thermocycler, the amplification time for 30 cycles is about 105 min. In the initial experiment using 1238 bp, an equal period of time of 20 s was set for denaturing, annealing, and extension zones with initial denaturation duration of 120 s, resulting in a total reaction time of 39.5 min. No visible bands were detected but more toward smearing [Fig. 6(a)] from the gel electrophoresis results of this initial experiment. The smearing confirms that either the denaturation time, extension time, or both are not adequate.

To ensure that denaturation and extension are properly completed, both were extended to 45 s. The total time required to complete this new amplification process is about 57 min including 55 min for 30 cycles of amplification and an initial denaturation of 2 min. This is only about a half of time used for the conventional PCR. Figure 6(b) shows the gel electrophoresis results of the second experiment with 1238 bp. The result confirms that an increase in denaturation and extension time significantly improves the amplification efficiency. Hence, a longer base pair DNA template requires much longer time for complete denaturation and extension to occur than a short pair of DNA template does.

## B. Inhibition and adsorption

Figures 7(a) and 7(b) show the gel electrophoresis of 150 and 1238 bp DNA template amplification results, respectively. Results from these preliminary tests to examine inhibition and adsorption illustrate that no apparent adsorption of template DNA took place in the glass PCR chip for both types of DNA templates tested. It was found that the length of incubation inside the chip does not affect the adsorption rate. It is now confirmed that the special coating of the channels can prevent molecule adsorption to the channel walls. Visual inspection of the electrophoresis slab gel shows that no significant changes appeared in the band intensity.

The possibility of *Taq* polymerase adsorption onto the chip walls was also assessed and the experiment was fairly conclusive. As seen from Fig. 8, the efficiency of the subsequent amplification does not differ to the time the PCR mix incubated inside the chip. It can be concluded that the fluorinated carbon coating of the channel walls is capable of avoiding *Taq* adsorption. Therefore, this PCR chip is PCR friendly in terms of DNA and *Taq* polymerase adsorption.

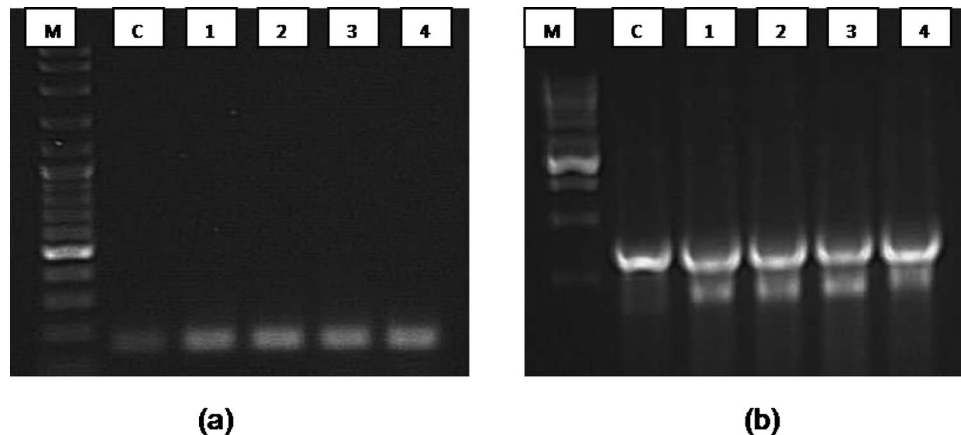


FIG. 7. Gel electrophoresis results of DNA adsorption experiment; (a) 150 bp DNA templates (lane M: 100 bp ladder; lane C: control; lanes 1–4: chip) and (b) 1238 bp DNA templates (lane M: 1 kbp ladder; lane C: control; lanes 1–4: chip).

### C. Bubbles formation and evaporation

As evaporation mainly occurred at the denaturing zone where the temperature is high (95 °C), the port near the denaturing zone was plugged. The channel was completely sealed as the other port was connected to the syringe pump. This significantly reduces the sample evaporation, even for samples processed in high temperature zones. Under standard atmospheric pressure, water evaporation is vigorous at 100 °C. The PCR samples evaporate rapidly in the previous designs once they are positioned in the denaturing zone due to its high temperature and also the opening of the outlet port to the atmosphere.

The loading point was deliberately designed near the lower temperature zone. Once the syringe pump starts operating, air is compressed into the channel to drive the sample plug toward the distal end of the channel where the temperature is high. Due to the increase in the pressure of the samples, the boiling temperature is also increased. Due to coupled effects of sealed environment and increased pressure inside the channel, the evaporation rate is only about 10% for an amplification process of 30 cycles (Fig. 9).

Another inherent problem related to the PCR chip is the formation of bubbles at high temperature. Figure 10(a) shows the various stages of bubble formation at different temperatures. The chip was placed on a temperature controllable hot plate and the bubble formation was observed. From the figure, it can be seen that the bubbles started to form when the chip temperature exceeded 90 °C.

The problem was solved by introducing a highly viscous mineral oil with a high boiling point

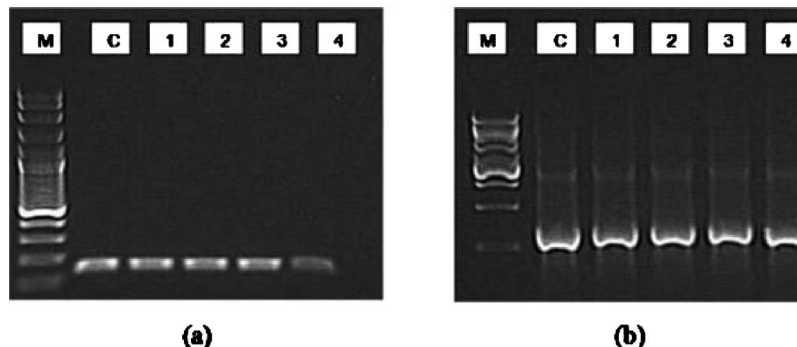


FIG. 8. *Taq* polymerase adsorption slab gel electrophoresis results. (a) 150 bp (lane M: 100 bp ladder; C: control; 1, 2, 3, 4: chip) and (b) 1238 bp (lane M: 1 kbp ladder; C: control; 1, 2, 3, 4: chip).

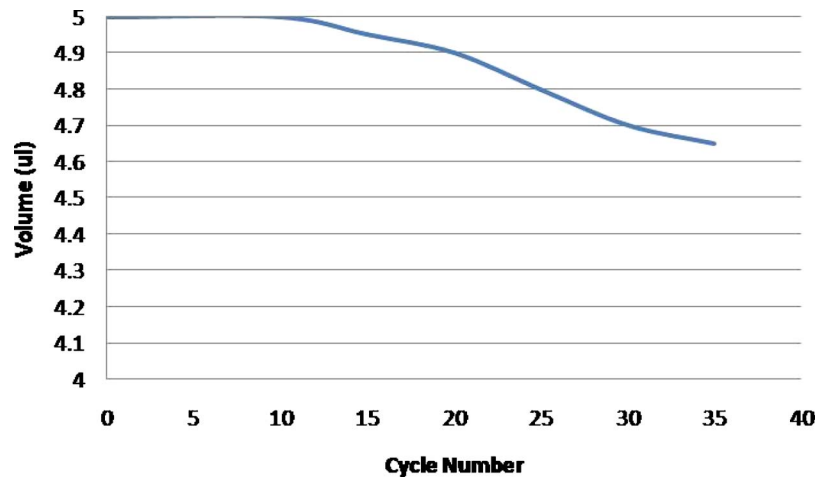


FIG. 9. Sample evaporation rate inside the PCR chip.

(Sigma Aldrich Light Mineral Oil M5904, USA) at the two ends of the DNA samples, applied before and after the PCR sample was injected into the microfluidic. The oil in return helped increase the pressure of the sample solution in the microchannels. The sample plug was basically “sealed” with light mineral oil, which prevents the formation of bubbles. In this method,  $1 \mu\text{l}$  of the oil was inserted into the chip with a micropipette prior and after injecting the PCR samples. Oil plugs in front and at the back of the sample solution that increase the internal pressure of the sample solution, provided a stable microfluidic flow. Figure 10(b) shows the stability of the sample plug even at high temperatures. The addition of oil plugs also reduces the sample evaporation rate from the chip. It was found that the majority of sample loss was during sample extraction after the amplification.

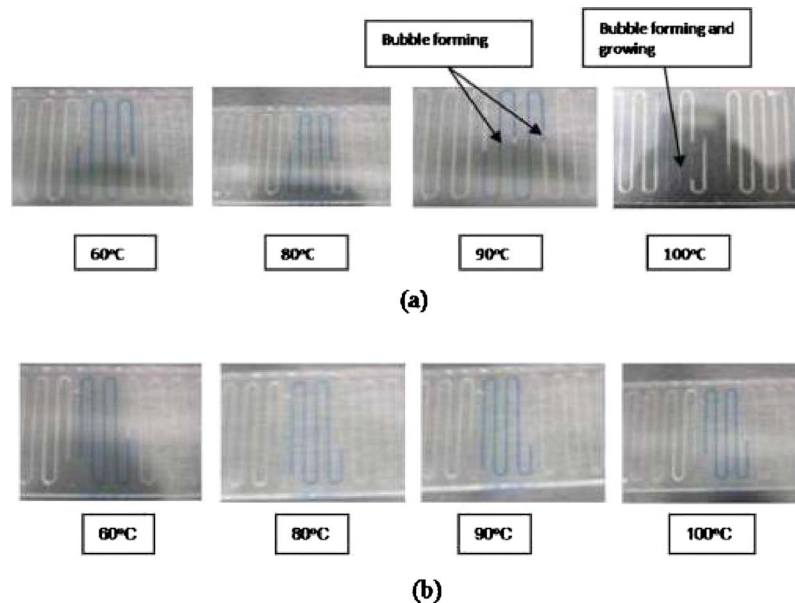


FIG. 10. (a) Formation of bubbles inside the microchannels at various temperatures without oil plug. (b) Absence of bubbles inside the microchannel even at high temperatures with the addition of oil plug.

## V. CONCLUSION

In this paper, an oscillating flow design is introduced for DNA amplification using PCR. The results showed that the design is able to successfully amplify 150 and 1238 bp DNA templates. For the 150 bp DNA template, the total time required for 30 cycles was only 29.5 min, less than one-third of the 90 min required for a conventional thermal cycler. As 1238 bp DNA templates, the total cycle time was about 55 min, about a half of the 105 min by a conventional thermal cycler. The issues related to inhibition and adsorption of DNA and *Taq* polymerase were also investigated and no apparent inhibition or adsorption issues were present on the chip. The bubble formation and sample loss from evaporation have been alleviated through the introduction of mineral oil to the two ends of the sample in the microchannel.

- <sup>1</sup>L. X. Kong, Z. Peng, and D. Sugumar, *J. Nanosci. Nanotechnol.* **6**, 2754 (2006).
- <sup>2</sup>M. W. Lassner, P. I. Peterson, and J. Yoder, *Plant Molecular Biology Reporter* **7**, 116 (1989), <http://www.springerlink.com/content/x37606116v026431>.
- <sup>3</sup>S. P. Johnston, N. J. Pieniazek, M. V. Xayavong, S. B. Slemenda, P. P. Wilkins, and A. J. da Silva, *J. Clin. Microbiol.* **44**, 1087 (2006).
- <sup>4</sup>C. Poyart, A. Tazi, H. Reglier-Poupet, A. Billoet, N. Tavares, J. Raymond, and P. Trieu-Cuot, *J. Clin. Microbiol.* **45**, 1985 (2007).
- <sup>5</sup>C. T. Wittwer and D. J. Garling, *BioTechniques* **10**, 76 (1991).
- <sup>6</sup>P. Wilding, M. A. Shoffner, and L. J. Kricka, *Clin. Chem.* **40**, 1815 (1994).
- <sup>7</sup>I. Schneegaß, R. Bräutigam, and J. M. Köhler, *Lab Chip* **1**, 42 (2001).
- <sup>8</sup>L. Kricka and P. Wilding, *Anal. Bioanal. Chem.* **377**, 820 (2003).
- <sup>9</sup>P. Belgrader, W. Benett, D. Hadley, J. Richards, P. Stratton, R. Mariella, Jr., and F. Milanovich, *Science* **284**, 449 (1999).
- <sup>10</sup>M. U. Kopp, A. J. d. Mello, and A. Manz, *Science* **280**, 1046 (1998).
- <sup>11</sup>C. T. Wittwer, G. C. Fillmore, and D. R. Hillyard, *Nucleic Acids Res.* **17**, 4353 (1989).
- <sup>12</sup>M. A. Northrup, C. Gonzalez, D. Hadley, R. F. Hills, P. Landre, S. Lehew, R. Saw, J. J. Sninsky, and R. Watson, The Eighth International Conference on Solid-State Sensors and Actuators, 1995 and Eurosensors IX. Transducers '95, 1995.
- <sup>13</sup>M. A. Shoffner, J. Cheng, G. E. Hvichia, L. J. Kricka, and P. Wilding, *Nucleic Acids Res.* **24**, 375 (1996).
- <sup>14</sup>X. Chen, D. Cui, C. Liu, H. Li, and J. Chen, *Anal. Chim. Acta* **584**, 237 (2007).
- <sup>15</sup>P. J. Obeid and T. K. Christopoulos, *Anal. Chim. Acta* **494**, 1 (2003).
- <sup>16</sup>S. Li, D. Y. Fozdar, M. F. Ali, L. Hao, S. Dongbing, D. M. Vykoukal, J. Vykoukal, P. N. Floriano, M. Olsen, J. T. McDevitt, P. R. C. Gascoyne, and C. Shaochen, *J. Microelectromech. Syst.* **15**, 223 (2006).
- <sup>17</sup>T. B. Taylor, S. E. Harvey, M. Albin, L. Lebak, Y. Ning, I. Mowat, T. Schuerlein, and E. Principe, *Biomed. Microdevices* **1**, 65 (1998).
- <sup>18</sup>W. Wang, H.-B. Wang, Z.-X. Li, and Z.-Y. Guo, *J. Biomed. Mater. Res. Part A* **77A**, 28 (2005).
- <sup>19</sup>N. J. Panaro, X. J. Lou, P. Fortina, L. J. Kricka, and P. Wilding, *Biomed. Microdevices* **6**, 75 (2004).
- <sup>20</sup>J. D. Cox, M. S. Curry, S. K. Skirboll, P. L. Gourley, and D. Y. Sasaki, *Biomaterials* **23**, 929 (2002).
- <sup>21</sup>H. Gong, N. Ramalingam, L. Chen, J. Che, Q. Wang, Y. Wang, X. Yang, P. Yap, and C. Neo, *Biomed. Microdevices* **8**, 167 (2006).